

# Influence of Bi Addition on Pure Sn Solder Joints: Interfacial Reaction, Growth Behavior and Thermal Behavior

LAI Yanqing, HU Xiaowu\*, LI Yulong, JIANG Xiongxin

(Key Lab for Robot & Welding Automation of Jiangxi Province, Mechanical & Electrical Engineering School, Nanchang University, Nanchang 330031, China)

**Abstract:** The effects of different Bi contents on the properties of Sn solders were studied. The interfacial reaction and growth behavior of intermetallic compounds (IMCs) layer ( $\eta$ -Cu<sub>6</sub>Sn<sub>5</sub> +  $\varepsilon$ -Cu<sub>3</sub>Sn) for various soldering time and the influence of Bi addition on the thermal behavior of Sn-xBi solder alloys were investigated. The Cu<sub>6</sub>Sn<sub>5</sub> IMC could be observed as long as the molten solder contacted with the Cu substrate. However, with the longer welding time such as 60 and 300 s, the Cu<sub>3</sub>Sn IMC was formed at the interface between Cu<sub>6</sub>Sn<sub>5</sub> and Cu substrate. With the increase of soldering time, the thickness of total IMCs increased, meanwhile, the grain size of Cu<sub>6</sub>Sn<sub>5</sub> also increased. An appropriate amount of Bi element was beneficial for the growth of total IMCs, but excessive Bi ( $\geq 5$  wt%) inhibited the growth of Cu<sub>6</sub>Sn<sub>5</sub> and Cu<sub>3</sub>Sn IMC in Sn-xBi/Cu microelectronic interconnects. Furthermore, with the Bi contents increasing (Sn-10Bi solder in this present investigation), some Bi particles accumulated at the interface between Cu<sub>6</sub>Sn<sub>5</sub> layer and the solder.

**Key words:** intermetallic compound; Sn-xBi solder joints; interfacial reaction; thermal behavior

## 1 Introduction

In recent decades, electronic packaging industry has made great achievements. However, as lead-based electronic products have caused serious pollution, the electronic packaging industry also calls for lots of pollution-free solders, more and more countries and regions have begun to pay attention to the development and research of the lead-free solders<sup>[1-3]</sup>. In recent decades, Lead-free solders have attracted a great deal of attention and made great progress such as Sn-Ag, Sn-Cu, Sn-Ag-Cu, Sn-Zn, Sn-In and Sn-Bi systems<sup>[4-8]</sup>. Among the various alternative lead-free solder systems, Sn-Bi alloy is one of the best substitutes to lead-containing solders<sup>[11]</sup>. It has not only a lower melting temperature (139 °C), but also a lower coefficient of thermal expansion<sup>[9,10]</sup>. Meanwhile, it has other

advantages, such as energy saving, reducing heat damage, good wettability and high creep resistance<sup>[12,13]</sup>.

The interfacial reaction between solder and metal substrate is a very important process, which is the key to determining the good metallurgical combination of the electronic interconnections<sup>[9,14,15]</sup>. As we all known, IMCs have a great influence on the firmness of the soldered joint due to the inherent hard and brittle nature of the IMCs, the formation of excess and thick intermetallic compounds (IMCs) can lead to decrease of the bond strength between solder and metallization<sup>[16]</sup>. The formation of IMCs during the soldering process also plays an important role in the wettability of the solder<sup>[17]</sup>. In the electronic packaging industry, the soldering time for the interfacial reaction from a few seconds to several minutes in most of researches<sup>[18]</sup>. There have some papers focused on the kinetics of IMC growth and interfacial reaction between Sn-xBi solders and Cu substrates<sup>[8,19]</sup>. An amount of investigations were studied about the growth behaviors and growth kinetics of the IMC. Additionally, the researches of the thermal behavior of SnBi solders are still lacking data. This study aimed at the interfacial reaction and the growth behavior of the IMC layer between Sn-xBi solders and Cu substrate during soldering with different time. The paper would further deepen the comprehension of the effect of Bismuth addition on

© Wuhan University of Technology and Springer-Verlag GmbH Germany, Part of Springer Nature 2019

(Received: June 18, 2018; Accepted: Jan. 25, 2019)

LAI Yanqing(赖彦青): E-mail: lyq5868@126.com

\*Corresponding author: HU Xiaowu (胡小武): Ph D; E-mail huxiaowu@ncu.edu.cn

Funded by the National Natural Science Foundation of China (No.51465039), Natural Science Foundation of Jiangxi Province (No.20151BAB206041, 20161BAB206122) and Fund of the State Key Laboratory of Solidification Processing in NWPU (No. SKLSP201508)

interfacial reaction between Sn-based solders and substrate. Moreover, we provide a reference for the growth behavior of IMCs between liquid SnBi solders and Cu substrate. Additionally, the influence of Bi addition on the thermal behavior of SnBi solders were also systematically investigated in this paper.

## 2 Experimental

The substrate was prepared from pure Cu plate (99.99 wt%) with dimensions of  $10 \times 10 \times 2$  mm<sup>3</sup> and the SnBi solders alloys were prepared by melting pure Sn, and Bi (with 99.99% purity) together in an Al<sub>2</sub>O<sub>3</sub> crucible put in a vacuum induction-furnace. In order to reduce the error generated by the experimental process, the furnace chamber was evacuated and purged with argon before the melting. The solder was then remelted at least three times to assure the uniformity of the composition. Finally, the solders was poured out and cooled to room temperature. The chemical ingredient of the different Sn-*x*Bi alloys was examined using inductive coupled plasma-optical emission spectrometry (ICP-OES), as shown in Table 1.

**Table 1** Chemical compositions of the different Sn-*x* Bi solder alloys.

Solder alloys	Mass contents of elements/%	
	Bi	Sn
Sn	0	Bal.
Sn05Bi	0.51	Bal.
Sn1Bi	1.02	Bal.
Sn5Bi	5.02	Bal.
Sn10Bi	10.01	Bal.

The thermal behavior of Sn-*x*Bi solders were studied by using a Netzsch STA 499C differential scanning calorimeter (DSC) instrument with a continuous scanning rate of 10 °C/min. The alloy samples were heated to 280 °C and then cooled to room temperature.

The pure Cu 99.99 (wt%) substrate was cut and ground with 400#, 800#, 1200#, 2000# SiC paper, then the Cu substrate were polished by using 0.1 μm polishing pastes and rinsed in pure water respectively. The experimental samples of SnBi/Cu couples were divided into five groups, and every group have four samples. The experimental samples were dipped into the molten solder at 280 °C for various soldering time, such as 5, 30, 60 and 300 s.

When the soldering process was finished, the experimental samples were cooled to room temperature,

and then the SnBi/Cu couples were prepared for observations on the cross sectional structure as well as the top view of the IMC morphology at the interface between SnBi solders and Cu substrate under a FEI Quanta 200F scanning electron microscope (SEM) at a voltage of 20 keV.

The ordinary metallographic practice was used to observe the microstructure of cross-section. The etchant of 2%HCl+5%HNO<sub>3</sub>+93%CH<sub>3</sub>OH was prepared to observe the view of cross-section. Moreover, the top-view morphology of the IMC particles was revealed by deep etching to the solder joint with 10% HNO<sub>3</sub> and 90% distilled H<sub>2</sub>O at room temperature for 5 min in order to remove the remaining solder.

The image analysis software was used to calculate the area and length of IMCs layer from cross sectional SEM images. And the IMC grains size of Cu<sub>6</sub>Sn<sub>5</sub> were calculated from the top-view micrograph by using the image analysis software too. The average thickness of IMCs layer (*T*) was calculated for using measured area (*S*) divided by length(*L*) in the area. Each sample was measured at least ten locations. The obtained thickness of the IMCs layer is the average value of more than 10 measurements. The total thickness (*T*<sub>IMC</sub>) of the interfacial layer was shown by the following equation, the same equation is used for the thickness of the individual IMC layer:

$$T_{\text{IMC}} = S/L \quad (1)$$

## 3 Results and discussion

Fig.1 shows the DSC exothermic and endothermic peaks of the different Sn-*x*Bi solder alloys upon heating and cooling, as well as the results are concluded in Tables 2 and 3. Table 2 reveals that the addition of Bi have influence on the liquidus temperature (*T*<sub>peak</sub>), solidus temperature (*T*<sub>onset</sub>) and melting range of Sn-*x*Bi solders during the melting process. The melting ranges of SnBi alloys have obviously increase with

**Table 2** Solidus temperature (*T*<sub>onset</sub>) and liquids temperature (*T*<sub>peak</sub>) for Sn-*x*Bi solderalloys during heating

Solder alloy /wt%	Heating <i>T</i> <sub>onset</sub> /°C	Cooling <i>T</i> <sub>onset</sub> /°C	Undercooling ( <i>T</i> <sub>heat</sub> - <i>T</i> <sub>cool</sub> )/°C
Sn	231.8	182.5	49.3
Sn05Bi	229.1	184.6	44.5
Sn1Bi	226.5	208.6	17.9
Sn5Bi	215.5	210.5	5
Sn10Bi	197.9	202.3	4.4

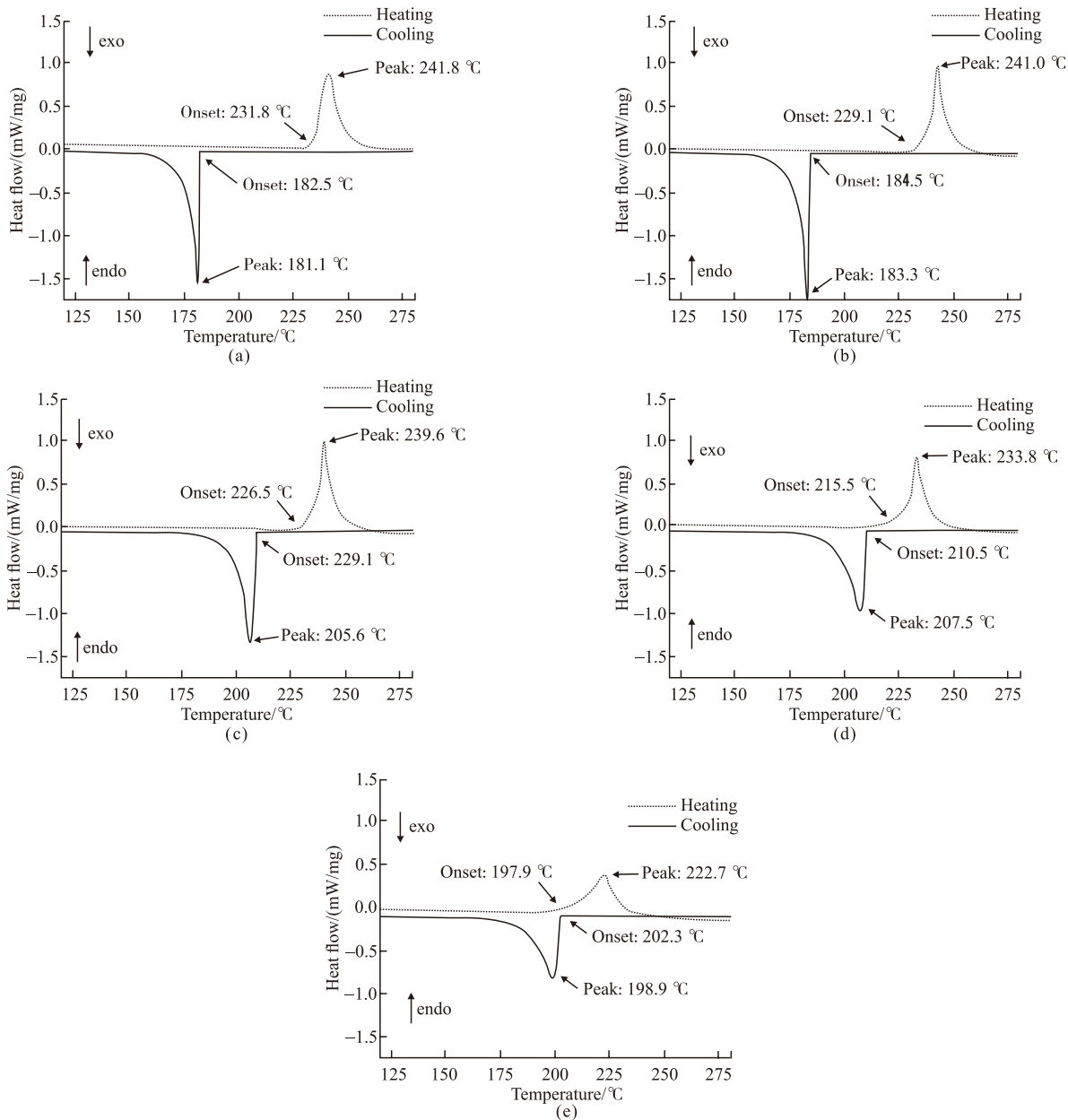


Fig.1 DSC results of Sn-xBi solder alloys: (a) Sn, (b) Sn-0.5Bi, (c) Sn-1Bi, (d) Sn-5Bi, (e) Sn-10Bi

the addition of bismuth. Besides, the solidification temperature of Sn solder increases with the increase of Bi content during the cooling process remarkably. The difference between the solidus temperature during heating ( $T_{\text{heat}}$ ) and the liquidus temperature during cooling ( $T_{\text{cool}}$ ) has been used to evaluate the undercooling of Sn-xBi solder alloys. It can be observed from Table 3 that the high undercooling value of the pure Sn solder significantly decreased from 49.3 to 4.4 °C with the addition of 10 wt% Bi element. More specifically, during the solidification process in the Sn-Bi system, the Bi particles are existed in the Sn matrix all the time, which can serve as extra heterogeneous nucleation sites, enhancing the rate of nucleation and

remarkably lowering the undercooling of solder alloys.

Fig.2 shows the SEM micrographs of cross-section view microstructures between Sn-0.5Bi solder

**Table 3 Comparison of solidus temperature ( $T_{\text{onset}}$ ) during heating, liquids temperature( $T_{\text{onset}}$ ) during cooling and undercooling range of Sn-x Bi solder alloys**

Solder alloy/wt%	Heating		Melting range /°C
	$T_{\text{onset}}/^{\circ}\text{C}$	$T_{\text{peak}}/^{\circ}\text{C}$	
Sn	231.8	241.8	10.0
Sn05Bi	229.1	241.0	11.9
Sn1Bi	226.5	239.6	13.1
Sn5Bi	215.5	233.8	18.3
Sn10Bi	197.9	222.7	24.8

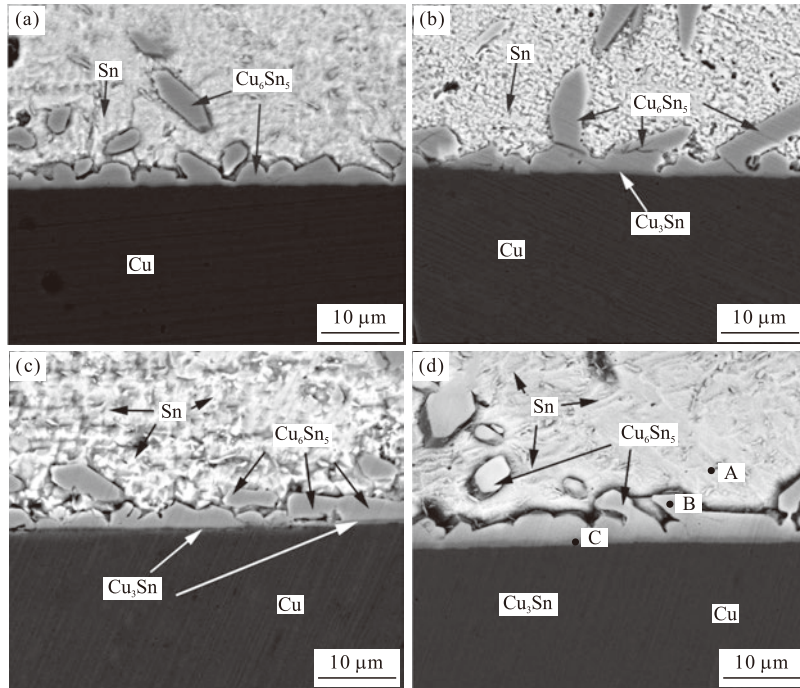


Fig.2 Cross-sectional views of the Sn-0.5Bi/Cu interface soldered at different soldering time for the same temperature of 280 °C: (a) 5 s; (b) 30 s; (c) 60 s; (d) 5 min

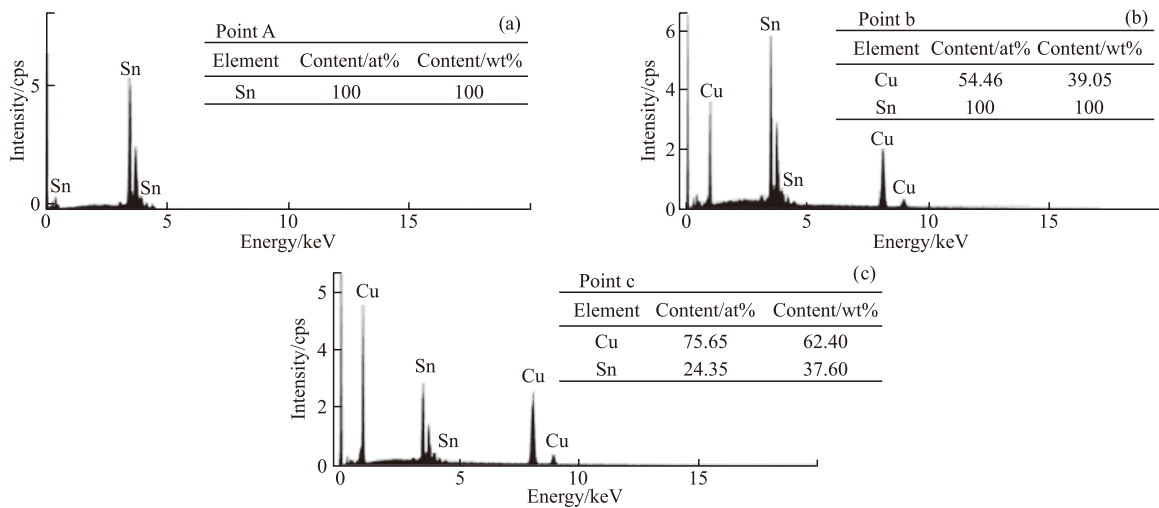


Fig.3 EDX analysis of IMCs between solder and Cu substrate: (a) EDX pattern of point A; (b) EDX pattern of point B; (c) EDX pattern of point C in Fig.2(d)

and Cu substrate after soldering for 5, 30, 60, 300 s at a constant temperature of 280 °C respectively. The soldered couples with soldering time of 5 s, the single layer of interfacial intermetallic compound (IMC) was discovered between the solder and Cu substrate. Meanwhile, two layers of interfacial intermetallic compound (IMCs) were detected when the soldering time increased to 30, 60 and 300 s, as shown in Fig.2(b)-2(d). In order to confirm the IMC phases between Cu substrate and solders by using Energy Dispersive X-ray Detector (EDX). The results of EDX were shown in Fig.3. Fig.3(a)-(c) corresponded to the EDX patterns of points A, B and C in Fig.2(e),

correspondingly. According to the test results of EDX, as shown in the Fig.3(a), the point A is determined to be Sn-rich phase, in Fig.3(b), the EDX result of point B reveals that the atomic percent ratio of Cu atoms and Sn atoms is close to 6 : 5, and the EDX result of point C shows that the atomic percent ratio of Cu atoms and Sn atoms is close to 3:1. According to the previous studies<sup>[20,21]</sup>, so the intermetallic phase of point B and point C can be estimated as Cu<sub>6</sub>Sn<sub>5</sub> phase and Cu<sub>3</sub>Sn phase, in other words, the layer of IMC near the Cu substrate is Cu<sub>3</sub>Sn, and the layer of IMC near Sn-xBi solder is Cu<sub>6</sub>Sn<sub>5</sub>, as shown in the Fig.2(b)-2(d), respectively.

As depicted in the Fig.2(b)-2(d), there are two layers near the Cu substrate, due to the  $\text{Cu}_6\text{Sn}_5$  IMC was formed firstly at the interface adjacent to the solder, and followed by the  $\text{Cu}_3\text{Sn}$  IMC formed between  $\text{Cu}_6\text{Sn}_5$  IMC the Cu substrate with higher soldering temperature<sup>[22,23]</sup>. Thus, the closest to the Cu substrate is  $\text{Cu}_3\text{Sn}$  IMC layer, which was distinguished from the other IMC by its gray level, the upper is  $\text{Cu}_6\text{Sn}_5$  IMC layer, the results are consistent with the result of EDX analysis. In this paper the  $\text{Cu}_3\text{Sn}$  IMC between  $\text{Cu}_6\text{Sn}_5$  IMC and Cu substrate was formed with longer soldering time.

The total thickness of IMC was 3.08, 3.57, 4.24, and 4.72  $\mu\text{m}$  and the thickness of  $\text{Cu}_6\text{Sn}_5$  IMC was 2.78, 3.08, 3.51, and 3.89  $\mu\text{m}$ , the thickness of IMC was 0.3, 0.49, 0.73, and 0.83  $\mu\text{m}$  respectively. Firstly,  $\text{Cu}_6\text{Sn}_5$  IMC was formed between the solder and Cu substrate followed by  $\text{Cu}_3\text{Sn}$  IMC formed adjacent to the Cu substrate with longer soldering time.

Fig.4 reveal the SEM micrographs of cross-section view microstructures between solders with various Bismuth contents and Cu substrate after soldering time of 60 s at a constant temperature of 280 °C individually. With the soldering time of 60 s the  $\text{Cu}_3\text{Sn}$  IMC was detected between the  $\text{Cu}_6\text{Sn}_5$  IMC and Cu substrate as shown in Fig.4(a)-4(e), the total thickness of IMC was 3.12, 4.24, 4.88, 3.92 and 3.88  $\mu\text{m}$  for various Bi additions. The interfacial IMCs layers between pure Sn solder and Cu Substrate were formed by the interaction

between the Sn atoms and Cu atoms from the solder and the substrate, respectively, which can be described by the following three equations<sup>[24]</sup>:



Generally speaking, the above referred consequence represented that  $\text{Cu}_6\text{Sn}_5$  IMC was formed firstly as long as the solder alloys contacted with Cu substrate, and the  $\text{Cu}_3\text{Sn}$  layer was developed between  $\text{Cu}_6\text{Sn}_5$  IMC and Cu substrate for the longer welding time.

Fig.5 shows the schematic diagram of the Bi segregation in the Sn-10Bi solder matrix and on the  $\text{Cu}_6\text{Sn}_5$  IMC surface. With the increasing of Bi contents (such as 10 wt%), the Bi segregated at the interface between solder and  $\text{Cu}_6\text{Sn}_5$ , which dramatically influenced on the mechanical properties of the solder/Cu joints. In the present investigation, lots of Bi particles can be discovered easily at the solder/ $\text{Cu}_6\text{Sn}_5$  interface of the Sn-10Bi/Cu couple soldered at 280 °C for 60 s, as depicted by the black arrows in Fig.4(e). In Reference[25], there was an assumption for the formation of Bi segregation. During the soldering process Bi segregation is mostly due to the diffusion of Bi atoms in the SnBi solder through the solder alloys. According to Reference[26], the solid solubility limit of

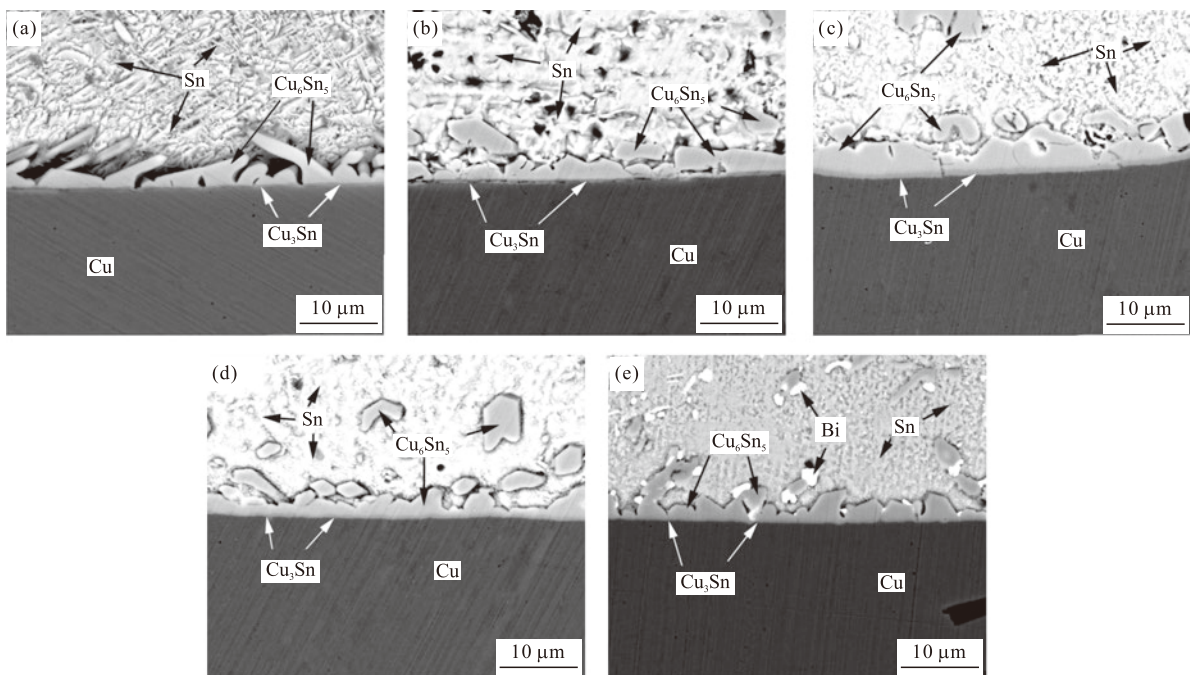


Fig.4 Cross-sectional views of the Sn-*x*Bi/Cu couples soldered of various Bismuth contents at 280 °C for one minute: (a) pure Sn; (b) Sn-0.5Bi; (c) Sn-1Bi; (d) Sn-5Bi; (e) Sn-10Bi

Bi in Sn at room temperature is about 1% from binary Sn-Bi phase diagram. Therefore, when the contents of Bi was saturated in this paper the diffusion of Bi atoms led to the formation of Bi segregation.

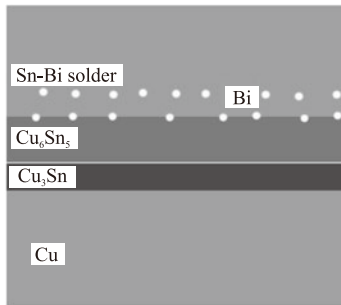


Fig.5 Schematic diagram of the Bi segregation in the Sn-10Bi solder and  $Cu_6Sn_5$  IMC surface

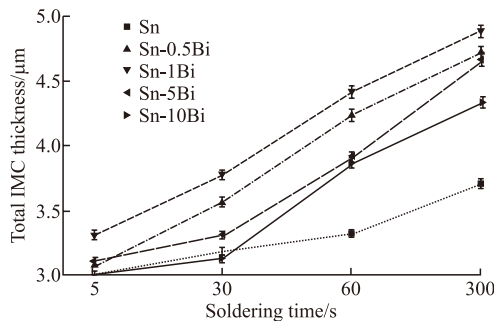


Fig.6 Average thickness of total IMCs layer of different Bismuth contents for different soldering time

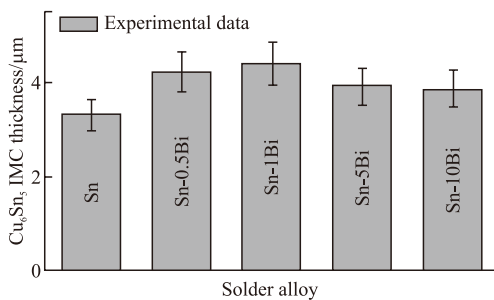


Fig.7 Average thickness of  $Cu_6Sn_5$  IMCs layer of different Bismuth contents for soldering time of one minute

In this study, Bi was added into the pure Sn solder. It is reported that the bismuth acted as a kind of catalyst in the process of interfacial reaction between Sn solder and Cu substrate, but it did not directly participate in the chemical reaction<sup>[27]</sup>. Therefore, the Cu-Sn reaction rate between Bi-containing Sn-based solders and Cu substrate is faster than that of the Sn/Cu interface. As well known, the chemical reaction includes many steps, such as atoms activation and metastable mid-reaction<sup>[28]</sup>. The addition of a small quantity of Bi can result in more chemical bonds between Cu and Cu atoms or Cu and Sn atoms to be broken, which leads to lots of Cu and Sn atoms activated<sup>[19,29]</sup>. Thus, the rates

of interfacial reaction described by Eqs.(2)-(4). When the Bi content was less than one percent, the thickness of the total IMC layer increased with increasing Bi contents. However, excessive Bi suppressed the growth of interfacial IMC and consumption of Cu substrate. According to the study of MJ Rizvi *et al*<sup>[30]</sup>, it was suggested that the Bi-addition into the solder resulted in lower interfacial reaction and lower Cu-consumption during soldering process between Sn-based solder and Cu substrate. Thus, excessive Bi restrained the growth of total IMCs.

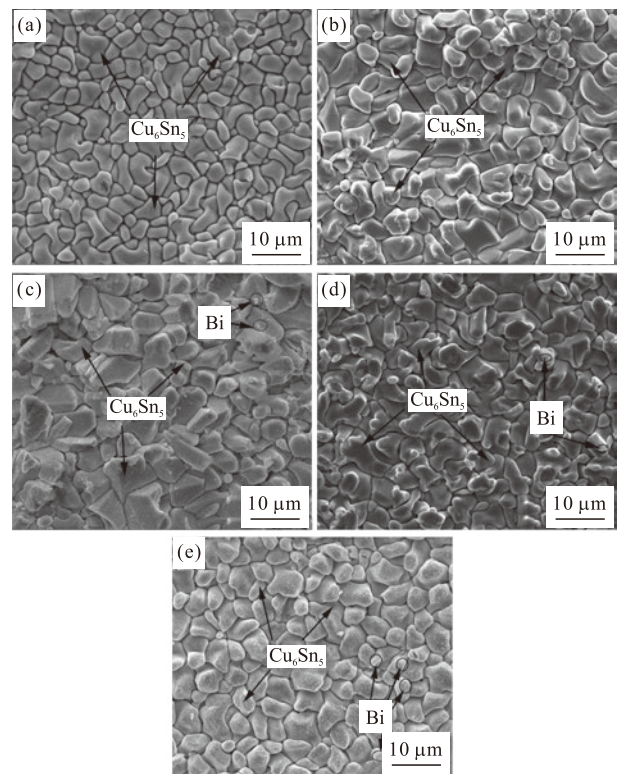


Fig.8 Top view of Sn-xBi/Cu interfacial  $Cu_6Sn_5$  grain reflowed at 280 °C of different bismuth contents for five minutes: (a) pure Sn; (b)Sn-0.5Bi; (c)Sn-1Bi; (d)Sn-5Bi; (e) Sn-10Bi

Fig.6 depicts the average thickness of total IMCs layer between solders with different Bismuth contents and Cu substrate after soldering at 280 °C for various time. It indicated that the average thickness of the total interfacial IMCs layer increased with increasing soldering time for all Sn-xBi/Cu solder joints. Compared with average thickness of total IMCs layer of Sn/Cu solder joints, the addition of the Bi contents increased the thickness of IMCs between Sn-xBi solders and Cu substrate. According to our previous results<sup>[19]</sup>, Bi atoms segregated at the  $Cu_3Sn$ /Cu interface accelerated the growth rate of  $Cu_6Sn_5$  IMC. With the Bi contents increasing, the thickness of the total IMCs layers increased firstly and then decreased.

Fig.7 shows the average thickness of  $\text{Cu}_6\text{Sn}_5$  IMCs layer between solders with different Bi contents and Cu substrate for soldering at 280 °C with 60 s. It indicates that the average thickness of  $\text{Cu}_6\text{Sn}_5$  of Sn-1Bi alloy was the thickest. For the pure Sn solder, in the solder-substrate interface the Cu-Sn intermetallic forms and increases due to continuous diffusion of Cu from the substrate into the solder matrix. Addition of 1 wt% Bi element into the pure Sn solder controls the nucleation of  $\text{Cu}_6\text{Sn}_5$  and  $\text{Cu}_3\text{Sn}$  intermetallics in the solder matrix during soldering condition.

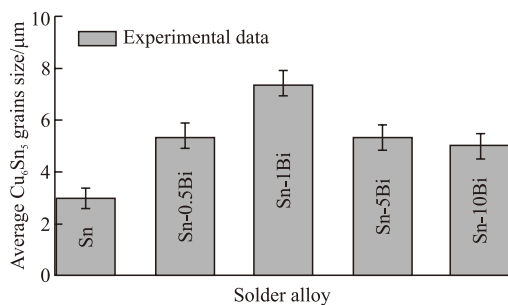


Fig.9 The average interfacial  $\text{Cu}_6\text{Sn}_5$  grain size of Sn-xBi/Cu joints soldered at 280 °C for 300 s

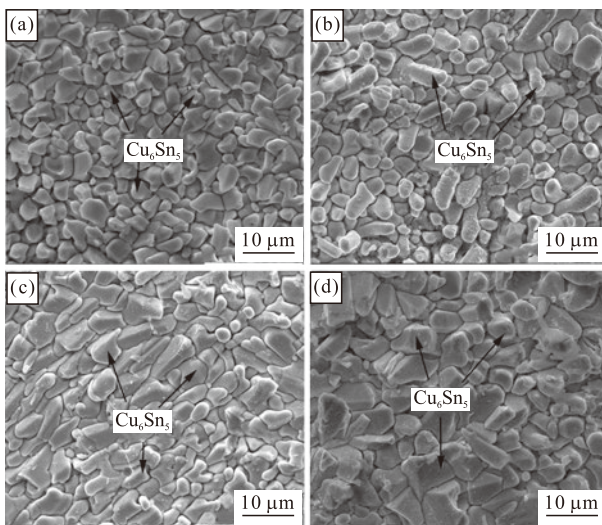


Fig.10 Top views of the Sn-1Bi/Cu couples soldered at 280 °C for various reaction time: (a) 5 s; (b) 30 s; (c) 60 s; (d) 300 s

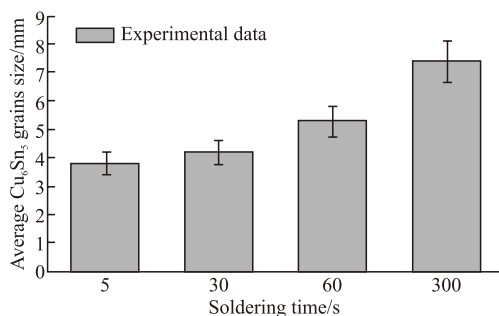


Fig.11 Average size of  $\text{Cu}_6\text{Sn}_5$  grains in Sn-1Bi/Cu solder joints for different soldering time

Fig.8 displays the top views of the Sn-xBi/Cu couples soldered at 280 °C for 300 s. In Figs.8(a), (b),

(c) and (d), the  $\text{Cu}_6\text{Sn}_5$  IMCs displayed faceted scallop-like morphology. While in Fig.8(e), a part of IMCs changed from hexagon scallop-type to spherical-type. Fig.9 shows that the average interfacial  $\text{Cu}_6\text{Sn}_5$  grain size of Sn-xBi/Cu joints soldered at 280 °C for 300 s. It can be clearly seen that the average interfacial  $\text{Cu}_6\text{Sn}_5$  grain size of Sn-xBi/Cu joints increases first and then decreases with the increasing of Bi contents.

Fig.10 presents the top-view of the Sn-1Bi/Cu couples soldered at 280 °C for various reaction time, which was confirmed as  $\text{Cu}_6\text{Sn}_5$  grains at the interface between the solder alloys and Cu substrate. Fig.10(a), (b) show scallop-like intermetallic compound grains of  $\text{Cu}_6\text{Sn}_5$ , (c) and (d) depict the prism-like intermetallic compounds, which can be detected in all soldered couples. Fig.11 indicates that the soldering time have an effect on the growth of Cu-Sn intermetallic compounds at the interface between Sn-1Bi solder and Cu substrate. Particularly, it illustrates that the grains size of the Cu-Sn IMCs increased with the increasing soldering time. In Reference[31], interfacial  $\text{Cu}_6\text{Sn}_5$  grains are enlarged with a prolonged soldering time, and in this investigation the experimental data is consistent with the result.

## 4 Conclusions

a) The high undercooling value of the SnBi alloys was markedly decreased from 49.3 to 4.4 °C with the addition of 10 wt% Bi. The melting range increased from 10 to 24.8 °C with the addition of 10 wt% Bi. Furthermore, it can be proved that the addition of Bi can lowered the melting points of the Sn-xBi solders.

b) Both thickness of total IMCs layer and  $\text{Cu}_6\text{Sn}_5$  grains size increased with increased soldering time. At the same soldering time when the Bi content was  $\geq 5$  wt%, Bi additions into the pure Sn solder suppressed the thickness of the Cu-Sn IMCs layer and controlled the nucleation of  $\text{Cu}_6\text{Sn}_5$  in the solder matrix and in the solder/substrate interface. Besides, both  $\text{Cu}_6\text{Sn}_5$  grains size and the thickness between solders and Cu substrate with different Bi contents exhibit a non-linear function with the soldering time.

c) Comparing with the thickness of total IMCs layer and the  $\text{Cu}_6\text{Sn}_5$  grains size of Sn-xBi/Cu joints at the same soldering time (such as 60 and 300 s), the samples of Sn-1Bi/Cu group possessed the thickest IMC layer and largest IMC grain among the all of Sn-xBi/Cu samples.

d) The excessive diffused Bi atoms resulted in Bi

accumulation at the interface between the solder and  $\text{Cu}_6\text{Sn}_5$  layer with the longer soldering time (such as 300 s), so that some isolated Bi particles were formed.

## References

- [1] Yang TL, Wu JY, Yang S, *et al.* Low Temperature Bonding for High Temperature Applications by Using SnBi Solders[J]. *Journal of Alloys and Compounds*, 2015, 647: 681-685
- [2] Zeng K, Tu KN. Six Cases of Reliability Study of Pb-free Solder Joints in Electronic Packaging Technology[J]. *Materials Science and Engineering*, 2002, 38: 55-105
- [3] Zhang L, Cui JH, Han JG, *et al.* Microstructures and Properties of SnZn-xEr Lead-free Solders[J]. *Journal of Rare Earths*, 2012, 30: 790-793
- [4] Tsai JY, Hu YC, Tsai CM, *et al.* A Study on the Reaction between Cu and Sn3.5Ag Solder Doped with Small Amounts of Ni[J]. *Journal of Electronic Materials*, 2003, 32: 1 203-1 208
- [5] Qu L, Zhao N, Zhao HJ, *et al.* In Situ Study of the Real-time Growth Behavior of  $\text{Cu}_6\text{Sn}_5$  at the Sn/Cu Interface During the Soldering Reaction[J]. *Scripta Materialia*, 2014, 72-73: 43-46
- [6] Wei XQ, Liao FP, Huang HZ, *et al.* Creep of Sn-9Zn as Measured by A Bending Test Method[J]. *Journal of Wuhan University of Technology-Mater. Sci. Ed.*, 2011, 04: 297-301
- [7] Nasir Bashir M, Haseeb A, Rahman AZMS, *et al.* Reduction of Electromigration Damage in SAC305 Solder Joints by Adding Ni Nanoparticles Through Flux Doping[J]. *Journal of Materials Science*, 2015, 50: 6 748-6 756
- [8] Hu XW, Chen WJ, Wu B. Microstructure and Tensile Properties of Sn-1Cu Lead-free Solder Alloy Produced by Directional Solidification[J]. *Materials Science and Engineering: A*, 2012, 556: 816-823
- [9] Yen YW, Liou WK, Chen CM, *et al.* Interfacial Reactions in the Sn-x Bi/Au Couples[J]. *Materials Chemistry and Physics*, 2011, 128: 233-237
- [10] Lin SK, Nguyen TL, Wu SC, *et al.* Effective Suppression of Interfacial Intermetallic Compound Growth between Sn-58 wt.% Bi Solders and Cu Substrates by Minor Ga Addition[J]. *Journal of Alloys and Compounds*, 2014, 586: 319-327
- [11] Tu XX, Yi DQ, Wu J, *et al.* Influence of Ce Addition on Sn-3.0Ag-0.5Cu Solder Joints: Thermal Behavior, Microstructure and Mechanical Properties[J]. *Journal of Alloys and Compounds*, 2017, 698: 317-328
- [12] Liu JC, Zhang G, Wang ZH, *et al.* Thermal Property, Wettability and Interfacial Characterization of Novel Sn-Zn-Bi-In Alloys as Low-temperature Lead-free Solders[J]. *Materials & Design*, 2015, 84: 331-339
- [13] Zhang L, Yang F. New Discovery of ZnO Whisker in SnZn/Cu Solder Joints Interconnection in Concentrator Silicon Solar Cells Solder Layer[J]. *Materials Letters*, 2016, 171: 154-157
- [14] Yao Y, Zhou J, Xue F, *et al.* Interfacial Structure and Growth Kinetics of Intermetallic Compounds between Sn-3.5Ag Solder and Al Substrate during Solder Process[J]. *Journal of Alloys and Compounds*, 2016, 682: 627-633
- [15] Yao Y, Fry J, Fine ME, *et al.* The Wiedemann-Franz-Lorenz relation for Lead-free Solder and Intermetallic Materials[J]. *Acta Materialia*, 2013, 61: 1 525-1 536
- [16] Yang M, Yang SH, Ji HJ, *et al.* Microstructure Evolution, Interfacial Reaction and Mechanical Properties of Lead-free Solder Bump Prepared by Induction Heating Method[J]. *Journal of Materials Processing Technology*, 2016, 236: 84-92
- [17] Wang YW, Lin YW, Kao CR. Inhibiting the Formation of Microvoids in  $\text{Cu}_3\text{Sn}$  by Additions of Cu to Solders[J]. *Journal of Alloys and Compounds*, 2010, 493: 233-239
- [18] Shen J, Pu YY, Yin HG, *et al.* Effects of Minor Cu and Zn Additions on the Thermal, Microstructure and Tensile Properties of Sn-Bi-based Solder Alloys[J]. *Journal of Alloys and Compounds*, 2014, 614: 63-70
- [19] Hu XW, Li YL, Li K, *et al.* Effect of Bi Segregation on the Asymmetrical Growth of Cu-Sn Intermetallic Compounds in Cu/Sn-58Bi/Cu Sandwich Solder Joints During Isothermal Aging[J]. *Journal of Electronic Materials*, 2013, 42: 3 567-3 572
- [20] Hu XW, Chen WJ, Yu X, *et al.* Shear Strengths and Fracture Behaviors of Cu/Sn37Pb/Cu Soldered Joints Subjected to Different Displacement Rates[J]. *Journal of Alloys and Compounds*, 2014, 600: 13-20
- [21] Li QQ, Chan YC. Growth Kinetics of the  $\text{Cu}_3\text{Sn}$  Phase and Void Formation of Sub-micrometre Solder Layers in Sn-Cu Binary and Cu-Sn-Cu Sandwich Structures[J]. *Journal of Alloys and Compounds*, 2013, 567: 47-53
- [22] Kang TY, Xiu YY, Liu CZ, *et al.* Bismuth Segregation Enhances Intermetallic Compound Growth in SnBi/Cu Microelectronic Interconnect[J]. *Journal of Alloys and Compounds*, 2011, 509: 1 785-1 789
- [23] Abdelhadi OM, Ladani L. IMC Growth of Sn-3.5Ag/Cu System: Combined Chemical Reaction and Diffusion Mechanisms[J]. *Journal of Alloys and Compounds*, 2012, 537: 87-99
- [24] Kang TY, Xiu YY, Liub CZ, *et al.* Bismuth Segregation Enhances Intermetallic Compound Growth in SnBi/Cu Microelectronic Interconnect[J]. *Journal of Alloys and Compounds*, 2011, 509: 1 785-1 789
- [25] Hu XW, Li YL, Min ZX. Interfacial Reaction and Growth Behavior of IMCs Layer between Sn-58Bi Solders and A Cu Substrate[J]. *Journal of Materials Science: Materials in Electronics*, 2013, 24: 2 027-2 034
- [26] Zhao J, Qi L, Wang XM, *et al.* Influence of Bi on Microstructures Evolution and Mechanical Properties in Sn-Ag-Cu Lead-free Solder[J]. *Journal of Alloys and Compounds*, 2004, 375: 196-201
- [27] Liang K, Tang XZ, Yu L, *et al.* Investigation of Preparation and Characteristics of Sn-Bi Eutectic Powders Derived from A High Shear Mechanical Approach[J]. *Journal of Alloys and Compounds*, 2011, 509: 9 823-9 841
- [28] Zou HF, Zhang QK, Zhang ZF. Interfacial Microstructure and Mechanical Properties of SnBi/Cu Joints by Alloying Cu Substrate[J]. *Materials Science and Engineering: A*, 2012, 532: 167-177
- [29] Huang ML, Yang YC, Chen Y, *et al.* Microstructure and Mechanical Properties of Sn-rich Au-Sn Solders Designed Using Cluster-plus-glue-atom Model[J]. *Materials Science and Engineering: A*, 2016, 664: 221-226
- [30] Rizvi MJ, Chan YC, Bailey C, *et al.* Effect of Adding 1 wt% Bi into The Sn-2.8Ag-0.5Cu Solder Alloy on The Intermetallic Formations with Cu-substrate during Soldering and Isothermal Aging[J]. *Journal of Alloys and Compounds*, 2006, 407: 208-214
- [31] Hu XW, Ke ZR. Growth Behavior of Interfacial Cu-Sn Intermetallic Compounds of Sn/Cu Reaction Couples during Dip Soldering and Aging[J]. *Journal of Materials Science: Materials in Electronics*, 2014, 25: 936-945